Available online at www.sciencedirect.com
ScienceDirect
Polymer 47 (2006) 8517–8526
polymer
www.elsevier.com/locate/polymer

Orientational order and mechanical properties of poly(amide-*block*-aramid) alternating block copolymer films and fibers

Christiaan de Ruijter [a], Eduardo Mendes [a], Hanneke Boerstoel [b], Stephen J. Picken [a,*]

[a] *Nanostructured Materials, Faculty of Applied Sciences, Delft University of Technology, Julianalaan 136, 2628 BL, Delft, The Netherlands*
[b] *Teijin Twaron B.V., Research Institute, P.O. Box 9300, 6800 SB Arnhem, The Netherlands*

Received 10 July 2006; received in revised form 5 October 2006; accepted 6 October 2006
Available online 2 November 2006

Abstract

Mechanical properties and orientational order of a series of uniaxially oriented block copolymer films and fibers comprised of alternating rigid aramid blocks of poly(*p*-phenylene terephthalamide) (PPTA) and flexible blocks of polyamide 6,6 (PA 6,6) have been investigated. The prepared block copolymer films differ in aramid content and average block length. The films were prepared by shearing the polymer solutions (in sulphuric acid) followed by rapid coagulation of the solutions in water. From wide angle X-ray scattering (WAXS) and optical polarisation microscopy (OPM) it was found that films with a mole fraction of PPTA of at least 0.5 show a liquid crystalline (LC) phase. It was found that the mechanical properties of LC block copolymer films are similar to the properties of isotropic films, as determined with dynamical mechanical analyses (DMAs) and from tensile tests. This was attributed to the relative low $\overline{\langle P_2 \rangle}$ parameter of the LC films obtained by using WAXS. Copolymerisation of the PPTA blocks with the flexible polyamide blocks resulted in an increase of storage and Young's modulus, a decrease of the elongation at break while the tensile strength was unaffected compared to normal PA 6,6. Block copolymer fibers have been spun from liquid crystalline solutions by means of a dry-jet wet spinning process. The only variable parameter was the imposed draw-ratio in the air-gap of the spinning process. Increasing the draw-ratio resulted in an increased molecular orientation, Young's modulus and tensile strength of the fibers while its effect on the maximum elongation at break was small. Heat treatment at 300 °C of the fibers resulted in an increase of the Young's modulus, a minor increase of the strength and a decrease of the elongation at break. Scanning electron microscopic (SEM) photographs of the fractured surfaces of the block copolymer fibers do not show a fibrillar fracture surface, which is typically observed for pure PPTA fibers.

Keywords: Block copolymers; Liquid crystalline polymers; Fibers

1. Introduction

Lyotropic main-chain liquid crystalline polymers are of great technological importance because of the high strength and high stiffness fibers that can be spun from liquid crystalline solutions by using a wet spinning process. The aramid polymer poly(*p*-phenylene terephthalamide) (PPTA) is, from a commercial point of view, the most important and is sold under trade names Twaron® and Kevlar®, by Teijin and Dupont, respectively. PPTA and other rigid aramids have been copolymerised with semi-flexible aramids or aliphatic amides to produce liquid crystalline block copolyamides. The purpose of attaching flexible blocks to rigid aramid blocks was either to improve the solubility [1–4] or melting behaviour (i.e. introduce thermotropic LC behaviour) [5], or to optimise the overall mechanical properties [6–8]. These block copolymers are able to form liquid crystalline solutions if the fraction and block length of the rigid component is large enough. In a previous report [8] we have shown that lyotropic solutions in sulphuric acid of a block copolymer prepared from alternating PPTA and polyamide 6,6 (PA 6,6) blocks are tolerant for a considerable fraction of the aliphatic amide because the flexible PA 6,6 blocks are partially oriented and stretched by the mesophase and therefore also contribute to the liquid crystalline behaviour.

* Corresponding author. Fax: +31152787415.
E-mail address: s.j.picken@tnw.tudelft.nl (S.J. Picken).

0032-3861/$ - see front matter © 2006 Published by Elsevier Ltd.
doi:10.1016/j.polymer.2006.10.006

In the present article we want to study the effect of aramid content and block length of the block copolymers in relation to the observed orientational order and the resulting mechanical properties. Therefore, we have prepared aligned polymer films by shearing the polymer solutions followed by rapid coagulation of the solutions in water. Films have been prepared from both isotropic and concentrated LC solutions. Also the effect of the orientation on the overall mechanical properties of the copolymers will be discussed.

Next, we have prepared block copolymer fibers by means of a dry-jet wet spinning process. All prepared fibers had the same composition and the only variable parameter was the applied draw-ratio in the air-gap. Here, we report on the relation between the tensile properties and orientational order of fibers spun from liquid crystalline solutions of a PPTA–PA 6,6 block copolymer in sulphuric acid as a function of the imposed draw-ratio in the air-gap. The measured moduli will be compared to a mechanical model that relates the modulus of a fiber to the overall orientational order present.

The preparations of block copolyamide fibers, comprised of alternating rigid and flexible blocks, have been reported recently by Helgee and Flodin [6] and Goto et al. [9]. Helgee and Flodin [6] have prepared multiblock copolymers of rigid poly(4,4′-benzanilidylene-terephthalamide) (DABT) and poly(4,4′-diphenylsulphone terephthalamide) and fibers were spun from liquid crystalline solutions whereas Goto et al. [9] prepared fibers of a block copolymer of PPTA and poly(4,4′-diphenyl ether terephthalamide) from isotropic solutions. In these studies the mechanical properties were reported and the fractured surfaces were investigated, however, the influence of the draw-ratio on the mechanical properties was not reported.

2. Experimental

2.1. Synthesis

A series of four block copolymers composed of alternating blocks of PPTA (poly-*p*-phenylene terephthalamide) and PA 6,6 (polyamide 6,6) were synthesised by a two-step low temperature polycondensation procedure in *N*-methyl-2-pyrrolidinone (NMP) containing about 10 wt% $CaCl_2$, as described in a previous paper [7]. The chemical structure of a repeat unit of the block copolymer is shown in Fig. 1 and Table 1 summarizes some characteristics of the block copolymers. The standard PPTA and PA 6,6 are used as reference polymers, and are obtained from Teijin Twaron and DSM, respectively.

Table 1
Characteristics of the block copolymers

Polymer	$[\eta]_{inh}$[a] (dl/g)	M_w[b]	Amount of flexible (PA 6,6) block (mol%)	Number of repeat units of	
				PPTA m (−)[c]	PA n (−)[c]
P10-4	1.87	11 000	29	10	4
P10-10	1.71	11 200	50	10	10
P4-4	2.06	17 200	50	4	4
P4-10	1.05	N.M.	71	4	10

[a] Measured at a concentration of 0.5 g/dl in 96% H_2SO_4 at 30 °C.
[b] Polystyrene equivalent molar masses as obtained by using SEC [7] (N.M. = not measured).
[c] m and n refer to in Fig. 1 and is an average number of the repeat units based on stoichiometry.

2.2. Film preparation

The films were prepared by manually shearing a polymer solution in sulphuric acid of 50 °C between two microscopic slides and immediately coagulating the aligned solution in water. In this way the obtained orientation is 'frozen in' in the films. Films of PPTA and the copolymers were prepared from both isotropic (10 wt%) and birefringent (possibly) LC solutions (15 wt%). For copolymer sample **P4-10** a 17 wt% solution was used because a 15 wt% solution at 50 °C according to the phase diagram [8] was certainly isotropic. For PA 6,6 only one solution was prepared because PA 6,6 shows no LC phase. The coagulated films were thoroughly washed with water, neutralized using a $CaCO_3$ solution and once again washed with water. Subsequently the films were dried overnight in vacuum at 50 °C and hot pressed for a few seconds at 250 °C. The films were kept dry in a vacuum oven at 110 °C for an extended period of time before DMA and WAXS measurements and tensile tests were performed. The thickness of the films was about 100 μm. The applied shear rate (velocity/film thickness) was in the order of 100 s^{-1}. The applied shear strain is approximately 15 units of strain if we assume that the displacement of the slides is about 1 cm and the layer thickness of the (15%) solution is about 100/0.15–700 μm.

2.3. Fiber spinning

The spinning of the fibers was performed at small-scale with a dry-jet wet spinning set-up at the Teijin Twaron Research Institute. A **P10-10** copolymer was synthesised for the fiber spinning experiments. The inherent viscosity $[\eta]_{inh}$ of the copolymer measured at a concentration of 0.5 g/dl in sulphuric acid of 30 °C was 2.07 dl/g, corresponding to a M_w

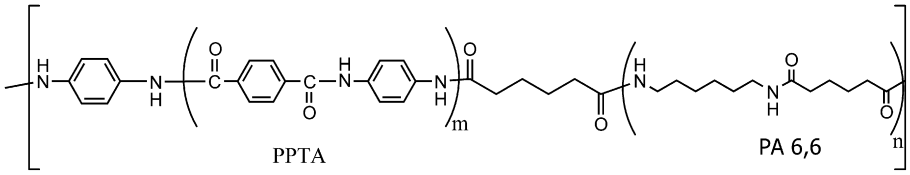

Fig. 1. Chemical structure of a repeating unit in the PPTA-*b*-PA-6,6 block copolymer.

of about 20 000 [7]. The polymer concentration in sulphuric acid of the spinning dope was 15 wt%. At this concentration the liquid crystalline solutions remain stable up to a temperature of about 100 °C [8]. The spinning temperature was about 60 °C. Fig. 2 schematically represents the experimental set-up for the dry-jet wet spinning process. The copolymer solution was extruded through a single hole spinneret (100 μm diameter) and stretched in the air-gap (6 mm) above the coagulation bath. The water in the coagulation bath was at room temperature. In the coagulation bath the sulphuric acid was removed and the fiber was formed. Finally the fiber was wound up at the take-up reel. During the spinning process the reel was kept at a constant speed. By adjusting the extrusion speed the draw-ratio in the air-gap was controlled. To ensure the complete removal of the sulphuric acid the reels were washed with water, a sodium hydroxide solution and finally again with water. A series of five fibers were prepared of which one had a draw-ratio smaller than 1. The maximum draw-ratio that could be applied during the spinning process without the frequent occurrence of fiber rupture was about 3.5.

2.4. Measurements

X-ray scattering experiments were performed on a Bruker-Nonius D8-Discover set-up with a 2D detector in order to estimate the orientational order of the polymer films and fibers. Monochromatic Cu Kα radiation with a wavelength of 0.154 nm was used. The direction of the incident X-ray beam was normal to the film surface and the molecular orientation via the (001) reflections was parallel to the film surface, i.e. along the shear direction. The detector–sample distance was set at 6 cm. The diffraction data was reordered using a 2 h exposure time and corrected for the background.

DMA measurements of the films were performed using a Perkin–Elmer DMA 7a apparatus. The temperature of the measurements was raised at a constant rate of 5 °C/min, from 25 to 350 °C, which is well above the melting point of the polyamide blocks. The measurements were performed on rectangular shaped films in tension along the shear direction. The frequency was 1 Hz.

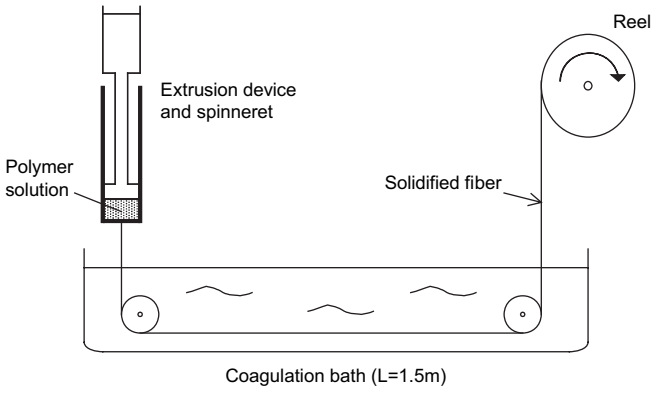

Fig. 2. Schematic drawing of the experimental set-up for the dry-jet wet spinning process.

The films were tested on a Zwick 1445 tensile tester with a 100 N force cell, equipped with a climate chamber. The films were tightened by hand between two grips with a rough surface to minimize slippage between the specimen and the grip. The test speed was 0.5 mm/min and the temperature was kept at 20 °C. For each type of film five samples were tested to determine the average values of the tensile properties.

The tensile tests of the polymer fibers were performed at the tensile test facility at Teijin Twaron in Arnhem (The Netherlands). All fibers were kept in an atmosphere of 65% relative humidity for at least 24 h before testing. The test speed was 10 mm/min and test temperature was 21.4 °C. Tensile tests were performed on a single filament. For each draw-ratio 10 filaments were tested to determine average values.

3. Results and discussions

3.1. WAXS measurements

3.1.1. Observed reflections

In Fig. 3, the 2-D X-ray scattering patterns of the diffraction of PPTA, PA 6,6 and the block copolymer films prepared from the most concentrated solutions are displayed. Fig. 4 shows the corresponding intensity curves as a function of the scattering angle 2θ. The films prepared from concentrated (15 wt%) solutions of PPTA, **P10-4**, **P10-10** and **P4-4** in sulphuric acid all displayed an anisotropic scattering pattern. In Fig. 5, the azimuthal scans of these polymers are shown. For all the other films, no significant anisotropy was observed from the azimuthal scans. This suggests that the corresponding precursor polymer solutions were not in a liquid crystal phase.

A 2D X-ray scattering pattern of the diffraction of **P10-10** fiber #4 is shown in Fig. 6. The fiber major axis is aligned at an angle of 45° with the vertical axis of figure. The corresponding intensity curve as a function of the scattering angle 2θ is shown in Fig. 7. All prepared fibers exhibit scattering peaks at nearly equal scattering angles, so only the pattern of one fiber is shown. The 2D scattering patterns differ only in the observed degree of alignment. The sharpness of the azimuthal peaks increases rapidly with increasing draw-ratio. The azimuthal profiles of the copolymer fibers are shown in Fig. 8.

The scattering patterns of the fibers differ to a certain extent from the films: the fibers exhibit both equatorial and meridional reflections, whereas the films show only equatorial reflections. At small scattering angles close to the beam stop reflections of moderate intensity are observed which can be attributed to the presence of phase-separated structures. These small-angle reflections are observed for all copolymer samples but are much more pronounced for **P4-10**, **P10-10**, and **P4-4** than for **P10-4** and the homopolymers (PPTA and PA 6,6). Another observation is that the relative intensity of this reflection of the fibers is higher than observed for the films, which suggests that the microphase separation in the fibers is more developed than in the films. From Fig. 3 it can be observed that the anisotropy of the peaks decreases with decreasing aramid content and is absent for copolymer sample **P4-10** and for pure PA 6,6. The diffraction spectra of these polymers show rings which are

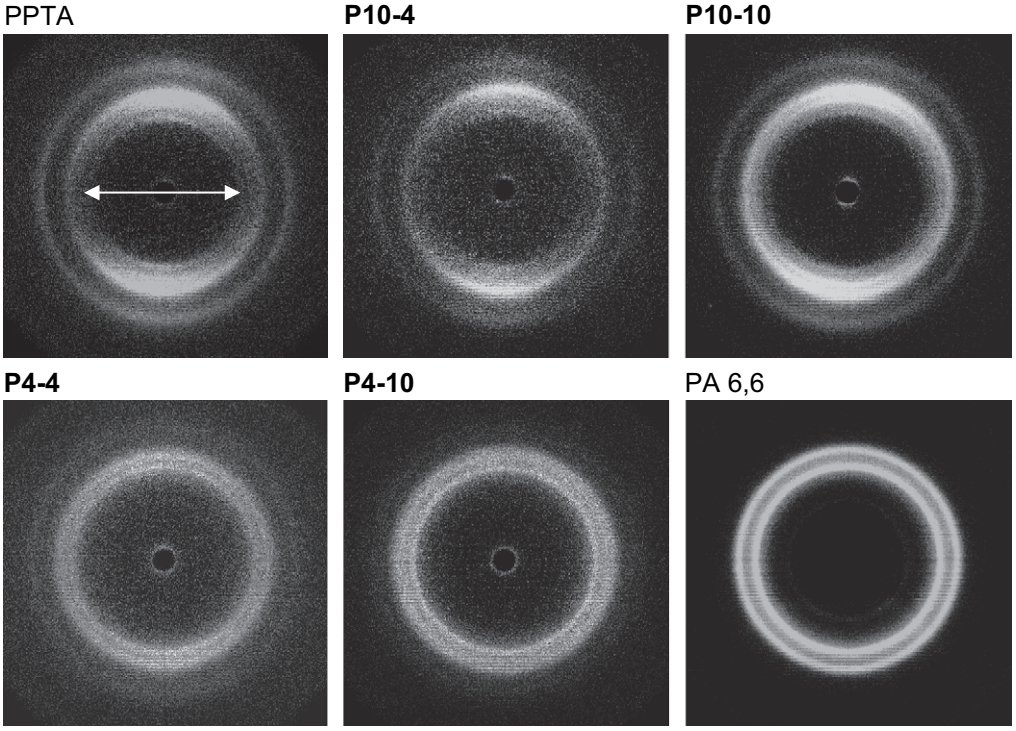

Fig. 3. 2D X-ray scattering patterns of the diffraction of the aligned polymer films of PPTA, **P10-4**, **P10-10**, **P4-4**, **P4-10** and PA 6,6 (the arrow reflects the direction of the shear flow).

uniform in intensity indicating no significant value of alignment. The d-spacings of observed reflections calculated according to Bragg's law for fiber #4 and the aligned polymer films are listed in Table 2. Also the d-spacings and the reflection indices of PPTA [10,11] fibers are listed in this table.

The diffraction pattern of the PPTA film shown in Fig. 3 corresponds mainly to the Haraguchi crystal structure [11]. Characteristics of this crystal structure are the reflections observed at a diffraction angle 2θ of 17.46°, 22.04° and 27.78° for, respectively, the (010), (200) and (211) planes [11]. But also a reflection at a diffraction angle of 20.73 is visible which corresponds to the (110) reflection of the Northolt crystal structure [10]. The Haraguchi crystal structure is transient crystal structure which is observed when PPTA is prepared from an isotropic or an anisotropic solution of low polymer concentration. Upon annealing the Haraguchi structure transforms into the Northolt structure. This process reveals itself by a gradual increase of the (110) reflection with increasing annealing temperature. The observed pattern of PA 6,6 shows sharp Debye rings for 2θ values of 13.55°, 20.45° and 23.75°

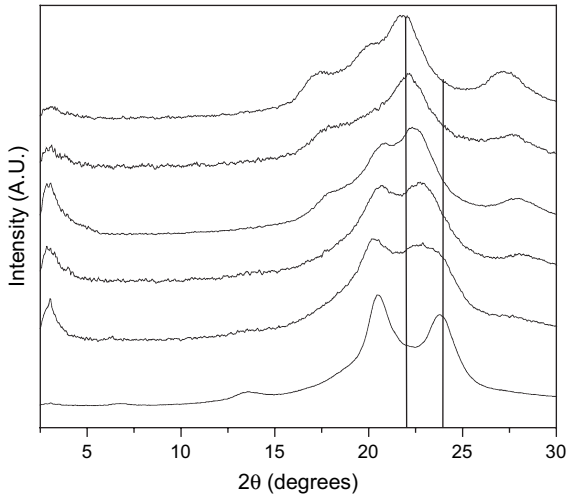

Fig. 4. Radial scattering intensity distribution of the aligned polymer films of PPTA, **P10-4**, **P10-10**, **P4-4**, **P4-10** and PA 6,6.

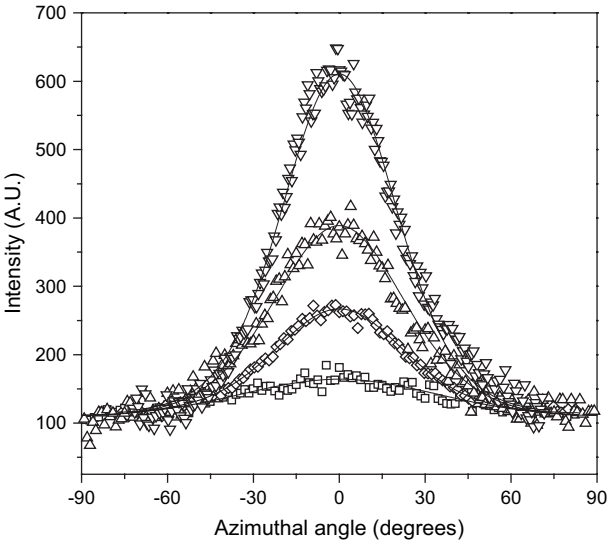

Fig. 5. Azimuthal profiles of PPTA and copolymer **P10-4**, **P10-10** and **P4-4** films obtained from 15 wt% solutions in sulphuric acid.

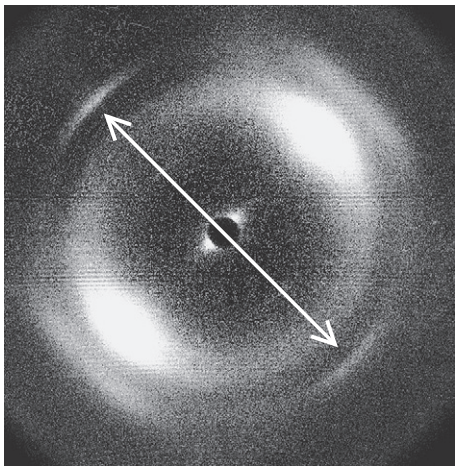

Fig. 6. 2D X-ray scattering pattern of the diffraction of block copolymer **P10-10** fiber #4 (the arrow represents the fiber direction).

corresponding to the (002), (100), and (010) planes of the triclinic α structure proposed by Bunn and Garner [12]. If we compare the diffractograms of the block copolymers with the pure components it striking that the intensity profile of block copolymers **P10-4** and **P10-10** resemble to great extent to the profile of PPTA. The sharpest reflection of all these polymers is the (200) reflection. Because of the partial overlap of the (200) PPTA and the PA 6,6 (010) reflections a gradual shift of this maximum is observed in $2\theta = 22-24^\circ$ range as is clear from the vertical lines drawn in Fig. 4. Because the hydrogen bonding sheets in the PPTA are forming the (200) lattice planes and the H-bonded sheets in PA 6,6 forming the (010) planes, this shift might be attributed to cross-hydrogen bonding between PPTA and PA 6,6. Another observation is that the intensity of the (211) aramid reflection indeed decreases with increasing polyamide content but remains constant with respect to the scattering angle. The most intense PA 6,6 reflection, the (100) reflection, becomes visible if the polyamide content is at least 50%. For copolymer **P4-10** this is the most intense observed reflection.

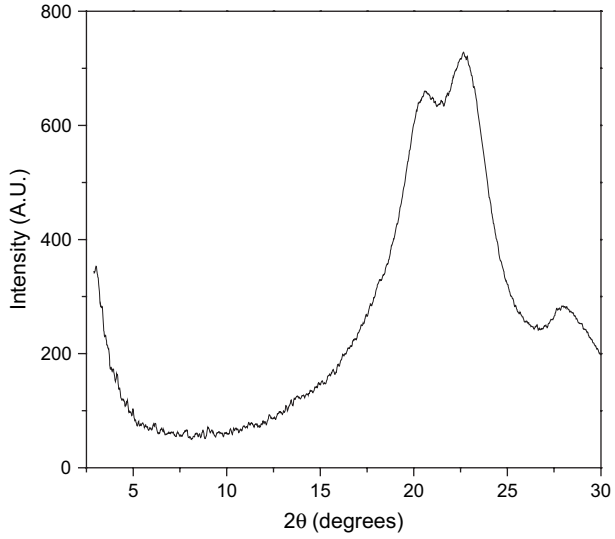

Fig. 7. Radial scattering intensity distribution of **P10-10** fiber #4.

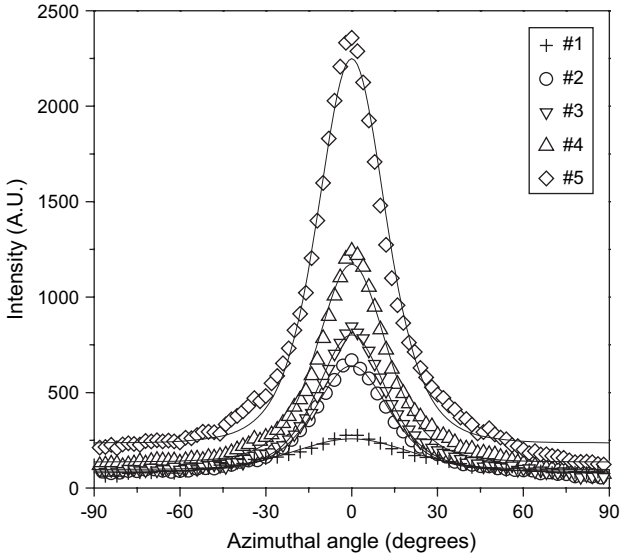

Fig. 8. Azimuthal profiles of the copolymer fibers.

The scattering pattern of the fibers largely corresponds to the Northolt crystal structure of PPTA [10]. A striking observation that can be drawn here is that the scattering pattern of the copolymer fiber shows great resemblance to the pattern of PPTA; also the observed d-spacings shown in Table 2 are very similar. This means that there is hardly any influence of the PA 6,6 on the scattering from the PPTA blocks, what indicates a well-developed phase separation of highly crystalline PPTA and amorphous PA.

3.1.2. Determination of the orientational order from the WAXS data

The experimental order parameter S_{exp} of a material can be estimated from an azimuthal integration over a single reflection in the scattering pattern. The experimental order parameter can be defined as a product of three contributions [13]:

$$S_{exp} = K\langle P_2\rangle \overline{P}_2 \quad (1)$$

where $\langle P_2\rangle$ is the local molecular order parameter, $\overline{P}_2$ is the macroscopic director order parameter and K is a parameter that describes azimuthal broadening of meridional reflections

Table 2
d-Spacings as obtained by WAXS of block copolymer **P10-10** film and fiber #4

d-Spacing **P10-10** fiber #4 (Å)	Intensity[a]	d-Spacing **P10-10** film (Å)	Intensity[a]	d-Spacing PPTA (Å)	Reflection indices for PPTA
3.02	w	3.21	m	3.02	211
3.09	m	–	–	3.23	004
3.92	vs	3.98	vs	3.94	200
4.22	s	4.25	s	4.33[b]	110[b]
–	–	5.02	w	5.0[c]	010[c]
6.23	vw	–	–	6.45	002

[a] Visually estimated intensities: vw – very weak, w – weak, m – medium, s – strong, vs – very strong.
[b] This reflection is observed only for the Northolt PPTA crystal [10].
[c] This reflection is observed only for the Haraguchi PPTA crystal [11].

due to translational disorder. If the integration is performed over an equatorial reflections the K factor is absent and Eq. (1) can be simplified to:

$$S_{\exp} = \langle P_2 \rangle \overline{P}_2 = \overline{\langle P_2 \rangle} \tag{2}$$

For normal PPTA fibers the orientational order is normally determined from the azimuthal profile of the (200) equatorial reflection [14,15]. The $\overline{\langle P_2 \rangle}$ order parameters of the polymer films considered here are also estimated from an azimuthal integration along the equatorial (200) reflection, which is the pattern with the highest peak intensity for the polymers PPTA, **P10-4**, **P10-10** and **P4-4** and is observed in the $2\theta = 22-23^\circ$ range. For the fibers an azimuthal scan around the (200), at 2θ is 22.7°, is performed. The intensity profiles an azimuthal peak can be fitted to a Maier–Saupe distribution function [16] with a free baseline I_0 and position of the maximum φ_0:

$$I = I_0 + A e^{\alpha \cos^2(\varphi - \varphi_0)} \tag{3}$$

where φ is the azimuthal angle and α is a parameter which determines the width of the distribution. From the α parameter the average orientational order parameter $\overline{\langle P_2 \rangle}$ is determined using:

$$\overline{\langle P_2 \rangle} = \frac{\int_{-1}^{1} P_2(\cos\varphi) e^{\alpha \cos^2\varphi} d\cos\varphi}{\int_{-1}^{1} e^{\alpha \cos^2\varphi} d\cos\varphi} \tag{4}$$

where $P_2(\cos\varphi)$ is the second order Legendre polynomial of $\cos(\varphi)$:

$$P_2(\cos\varphi) = \frac{1}{2}\left(3\cos^2\varphi - 1\right) \tag{5}$$

Eq. (4) is solved by a numerical integration. The obtained order parameters for all films are listed in Table 3. Results of the order parameter of the fibers as function of the draw-ratio are shown in Table 4.

Films prepared from concentrated (15 wt%) solutions of PPTA, **P10-4**, **P10-10** and **P4-4** in sulphuric acid all displayed an anisotropic scattering pattern. For all the other films, no significant anisotropy was observed from the azimuthal scans. This suggests that the corresponding precursor polymer solutions were not in a liquid crystal phase. Also, a concentrated (17 wt% in sulphuric acid) solution of sample **P4-10** which exhibited a slightly birefringent texture by OPM [8] does not seem to be in a LC phase because of the absence of an anisotropic azimuthal peak in the corresponding film. Therefore, the observed texture in this polymer might be related to microphase separation. From Table 3 and Fig. 5, it is clear that the sequence of the $\overline{\langle P_2 \rangle}$ values is PPTA > **P10-4** > **P10-10** > **P4-4** > **P4-10**. The orientational order is found to increase if the aramid content in the polymer increases, as anticipated. Also increasing the aramid block length increases the order parameter. This is clear from comparing samples **P10-10** and **P4-4**; the aramid content in the copolymers is the same but the $\overline{\langle P_2 \rangle}$ parameter of **P10-10** is distinctly higher. Although

Table 3
Order parameters and mechanical properties of the polymer films obtained by DMA and tensile tests

Polymer	Concentration in sulphuric acid (wt%)	$\overline{\langle P_2 \rangle}$ (−)	E′[a] (GPa) (30 °C)	E′[a] (GPa) (300 °C)	E[b] (GPa) (20 °C)	σ[c] (MPa) (20 °C)	ε[d] (%) (20 °C)
PPTA	15	0.51	6.2	3.5	7.1	90	1.5
	5	0	4.1	1.9	–	–	–
P10-4	15	0.47	4.3	1.7	5.6	83	3.6
	10	0	3.9	1.3	–	–	–
P10-10	15	0.36	2.8	0.8	4.5	75	4.4
	10	0	3.5	0.5	–	–	–
P4-4	15	0.16	3.6	0.4	3.7	71	3.7
	10	0	3.1	0.3	–	–	–
P4-10	17	0	1.8	0.08	2.7	79	7.1
	10	0	1.8	0.07	–	–	–
PA 6,6	20	0	1.7	0	2.0	81	10.6

[a] Storage modulus.
[b] Young's modulus.
[c] Tensile strength.
[d] Elongation at break.

Table 4
Order parameters and tensile properties of the fibers as a function of the draw-ratio

Fiber #	Draw-ratio (−)	$\overline{\langle P_2 \rangle}$ (−)	Initial modulus (GPa)	Modulus after yield (GPa)	Theoretical modulus (Eq. (5)) (GPa)	Tensile strength (MPa)	Elongation at break (%)	Toughness (J/g)
1	0.5	0.43	8.7	1.1	10.0	177	7.1	6.4
2	1.1	0.75	23.4	9.1	21.4	423	3.3	6.1
3	1.5	0.79	27.6	10.5	25.2	523	3.4	7.7
4	2.8	0.85	32.2	13.3	34.5	584	2.9	7.4
5	3.3	0.89	46.0	17.6	45.8	748	3.0	9.7

the copolymers with an aramid content of at least 50% display orientational ordering the value of the $\overline{\langle P_2 \rangle}$ parameters are rather small. This relatively low orientational order could be explained due to a significant degree of recoiling during the coagulation process. Also the films are rather thick and the coagulation rates are quite low this may cause inhomogeneous orientation in the film, i.e. only the polymer at the surface of the film is well aligned, in the remaining bulk the orientation could be lower.

Copolymer **P10-10** was chosen above the other copolymers to prepare the fibers because the phase separation was better developed compared to **P10-4** [8] and because polymer **P10-10** displays higher orientational order compared to **P4-4** and **P4-10**.

From Table 4 it is clear that the $\overline{\langle P_2 \rangle}$ parameter for the copolymer fibers rapidly increases with increasing draw-ratio, as anticipated. Also the observed orientations of the drawn fibers are significantly higher than that of the films. Another observation that can be made is that fiber #1 with a draw-ratio smaller than 1 already has a $\overline{\langle P_2 \rangle}$ value of 0.43. This indicates that the polymer is already somewhat aligned by the shear flow in the capillary and by the elongational flow above the entrance zone of the spinneret.

3.2. Mechanical properties of the copolymer films

Mechanical properties of the copolymer films were obtained by performing tensile tests and by dynamical mechanical analysis (DMA). Fig. 9 displays the storage modulus and Fig. 10 the loss modulus of the polymer films as a function of temperature. Fig. 11 displays the stress–strain curves of the polymer films as determined by tensile tests. The shown curves are all measured on the samples obtained from the most concentrated solutions. For these films we have shown using WAXS that PPTA, **P10-4**, **P10-10** and **P4-4** exhibit LC behaviour, while the **P4-10** and PA 6,6 films were isotropic. DMA

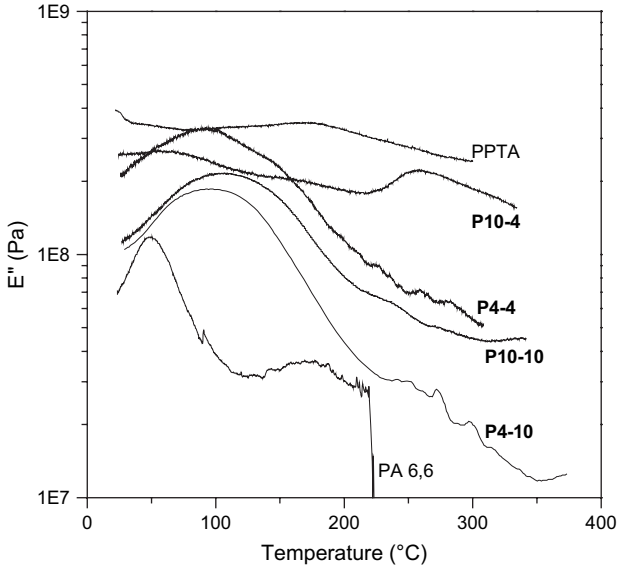

Fig. 10. Loss modulus of PPTA, **P10-4**, **P10-10**, **P4-4**, **P4-10** and PA 6,6.

curves obtained from the less concentrated (isotropic) solutions have also been measured but the differences in mechanical properties between LC and isotropic films turned out to be small. An explanation for this is that the orientational order of the LC films is not yet high enough for the mechanical properties to benefit from the LC alignment. Table 3 gives a schematic overview of the mechanical properties obtained by both methods (DMA and tensile tests). The storage modulus is reported both at ambient temperature as well as at 300 °C. Above that temperature, the modulus for the copolymer films remains more or less constant. Also, the Young's moduli, tensile strength and elongation at break are given in this table. As mentioned before the polymer concentration in sulphuric acid did not play a significant role for the mechanical properties according to DMA. Therefore, the tensile tests were only performed for the highest concentrations (see Table 3). In the

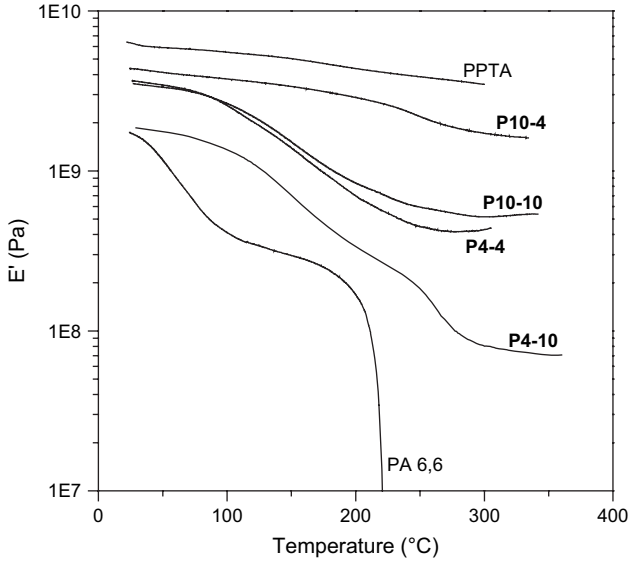

Fig. 9. Storage modulus of PPTA, **P10-4**, **P10-10**, **P4-4**, **P4-10** and PA 6,6.

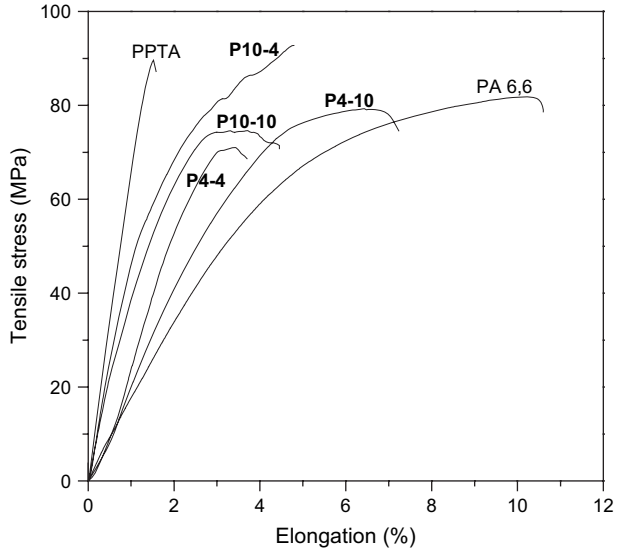

Fig. 11. Stress–strain curves of PPTA, **P10-4**, **P10-10**, **P4-4**, **P4-10** and PA 6,6.

following sections the results from DMA measurements and tensile tests are discussed more extensively.

3.2.1. Determination of temperature dependent mechanical properties of the films using DMA

Results of the DMA measurements are shown in Figs. 9 and 10. Fig. 9 displays the storage modulus as a function of temperature of the polymer films. The storage modulus of the polymers increases with increasing aramid content and decreases with increasing temperature, as anticipated. The largest drop in the modulus of the copolymers **P10-10**, **P4-4** and **P4-10** is between 120 and 150 °C which is considerably higher than the glass transition temperature of PA 6,6. At high temperatures (above ~280 °C) the modulus of all prepared copolymers shows a plateau value. This indicates the presence of a rubbery plateau above the melting point of the soft segments. This is a common feature for segmented block copolymers and therefore is a clear indication that a phase-separated block copolymer structure is formed. As a result, the structure of the copolymers can be envisaged as a covalent network where the rigid blocks act as crosslinked zones for the flexible blocks. Even copolymer sample **P4-10**, containing only 30% aramid, exhibits a plateau value above the melting point of the PA blocks of approximately 0.07 GPa. Since no sign of melting of the PPTA blocks is observed up to the degradation temperature of PA 6,6, which is around 400 °C, it is clear that none of the synthesised copolymers are expected to be melt-processable. On the other hand, since the mechanical properties of the block copolymers remain intact up to at least 400 °C high temperature applications of this material may be considered.

Fig. 10 displays the loss modulus versus temperature of the polymer films. The PA 6,6 sample exhibits a distinct peak at about 52 °C indicating the location of the glass transition temperature. The glass transition temperature for dry PA 6,6 reported in literature is 66 °C [17]. Also copolymer samples **P4-10**, **P4-4** and **P10-10** exhibit a peak corresponding to the T_g of PA 6,6 although the peak is much broader and is shifted to a higher temperature, around 120 °C. This shift towards a higher temperature can be explained by the reduced segmental mobility of the polyamide, which is constrained due to the presence of the rigid aramid blocks. Another observation that can be made from Fig. 10 is that copolymer **P10-4** exhibits a peak in the loss modulus around the melting temperature of the PA 6,6 blocks.

3.2.2. Determination of mechanical properties of the copolymer films by tensile testing

Tensile properties of the prepared polymer films are listed in Table 3 and the accompanying stress–strain curves of characteristic specimens are shown in Fig. 11. From Table 3 it is clear that with increasing aramid content in the copolymer, the initial Young's modulus gradually increases and the elongation at break gradually decreases, as expected. Another observation is that, in general, the obtained Young's moduli are somewhat higher than the storage moduli obtained by using DMA. The tensile strength of the polymer seems largely unaffected by the incorporation of aramids. The ultimate mechanical properties of course very much depend on the preparation method, although other factors like test conditions (temperature, humidity and test speed) may also play a major role. With our simple preparation method the samples are obviously not perfectly homogeneous and may suffer from voids and other structural imperfections. Nevertheless even using this simple preparation method the properties are quite promising. However, to obtain better mechanical properties a higher orientational order in the polymer is needed, i.e. a $\overline{\langle P_2 \rangle}$ value of about 0.8–0.9. To aim for such values of $\overline{\langle P_2 \rangle}$ for our materials, fibers of polymer **P10-10** have been prepared via a dry-jet wet spinning procedure. The relation between the orientational order and the modulus of the fibers is described next.

3.3. Mechanical properties of the copolymer fibers

3.3.1. Determination of mechanical properties of the fibers by tensile testing

Tensile properties of the spun fibers as a function of the imposed draw-ratio are listed in Table 4. The stress–strain curves for fiber #4 are shown in Fig. 12. From the stress–elongation curve three regimes can be specified. At small elongations a high initial modulus is observed that remains more or less constant up to 0.5% elongation. With increasing the deformation, the hydrogen bonds in the amorphous regions start to break, leading to the formation of a yield point while the initial modulus drops to almost 1/3 of its initial value. At deformations higher than 1.5% the modulus starts to increase with increasing deformation as the amorphous chains readily orient.

From Table 4 it is clear that with increasing draw-ratio the initial Young's modulus and the tensile strength rapidly increases. The elongation at break shows the tendency to decrease with increasing draw-ratio. Striking observations, which can be drawn from Table 4, are the impressive values for the Young's moduli of the fibers with a high draw-ratio. In a previous publication [8] we have already shown that the liquid crystallinity involves induced orientation of polyamide segments and therefore it is plausible that also the polyamide

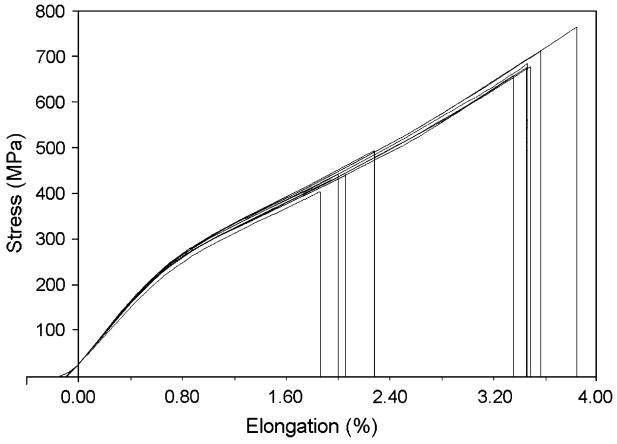

Fig. 12. Stress–elongation curve for fiber #4.

segment readily align upon the applied drawing and therefore contribute to the high value of the modulus. Based on the applied draw-ratio, the polymer concentration in sulphuric acid and the temperatures of the spinning dope and coagulation bath, the obtained moduli for the copolymers are in the order of what would be expected for pure PPTA [18].

In order to relate the obtained Young's moduli with the overall orientational order, which were obtained from WAXS measurements, the following mechanical model is used [19]:

$$\frac{1}{E} = \frac{1}{e_c} + \frac{1 - \overline{\langle P_2 \rangle}}{3g} \tag{6}$$

where E is the modulus of the fiber, e_c is the chain modulus and g the shear modulus. For PPTA the values for chain and shear moduli are, respectively, 240 [20] and 2 GPa [21]. According to Table 4 the initial moduli of the block copolymer fibers correspond rather well with the modulus calculated from the mechanical model of Northolt and Van der Hout [19] if shear and chain moduli of PPTA are chosen.

Although the tensile strength of the fibers considerably increases with increasing the draw-ratio, its value measured at even the highest draw-ratio, is still somewhat lower than the tensile strength of PA 6,6. The tensile strength of commercial PA 6,6 and PPTA fibers are, respectively, around 0.9 and 3 GPa [22]. It is commonly accepted that the tensile strength of high-performance fibers may be improved upon heat treatment. Heat treatment has been applied successfully to aromatic polyamide fibers and could even result in a two times improvement of both the modulus and tensile strength [23,24]. Fiber #4 was subjected to heat treatment at 300 °C and the results are shown in Table 5. Table 5 clearly shows that the Young's modulus drastically increases upon heat treatment and that the elongation at break decreases compared to untreated fibers. The tensile strength only slightly increases upon heat treatment. Similar results have been obtained by the groups of Helgee and Flodin [6] and Goto et al. [9] who also have investigated the mechanical properties of alternating rigid-flexible block copolyamide fibers. Tensile tests of their copolymers indicated a significant decrease of the tensile strength compared to the rigid homopolymer. Also only little influence of heat treatment on the fiber strength of the copolymer was observed, whereas for the rigid homopolymer the modulus drastically increases upon heat treatment. These are clear indications that the phase-separated morphology in the fibers contributes to the relatively low strength of the copolymer fibers. In order to further investigate this relative low strength compared to pure PPTA, the fracture morphology of the fibers was investigated by scanning electron microscopy (SEM). Fig. 13 shows the fracture surfaces of a PPTA and a block copolymer fiber, which were prepared by the same spinning procedure. From these photographs it is clear that a PPTA fiber has a much stronger tendency to form a fibrillar fracture surface. Because the block copolymers phase separates into small domains it loses the tendency to form these fibrils during breakage and probably a premature tensile rupture will occur.

Table 5
Effect of heat treatment on fiber properties

Fiber #	Draw-ratio (−)	Initial modulus (GPa)	Modulus after yield (GPa)	Tensile strength (MPa)	Elongation at break (%)	Toughness (J/g)
4	2.6	32.5	13.2	738	4.2	12.5
4 Heat-treated	2.9	55.0	29.2	811	2.0	6.7

Although the mechanical properties of the prepared fibers are already quite promising, additional improvement might be expected upon adjusting some of the spinning parameters. A range of parameters are known that can influence the ultimate mechanical properties of fibers prepared via a dry-jet wet spinning process, like e.g. the spinning dope temperature, the coagulation-bath temperature, the polymer concentration, the draw-ratio, the gap size of the spinneret and the size of the air-gap. In our view, a significant improvement of the mechanical properties might be expected by increasing the polymer concentration of the spinning dope, since a higher concentration allows for a higher draw-ratio and the polymer concentration of the spinning dope used was relatively low (15 wt%) compared to the solubility limit which is about 25 wt%. For pure PPTA it is known that the fiber strength approximately doubles if the polymer concentration is doubled [25], which means that probably also for the copolymer an increase in fiber strength can be expected. Another factor that might improve the fiber strength is increasing the block length. By increasing the block length the extent of microphase separation will be

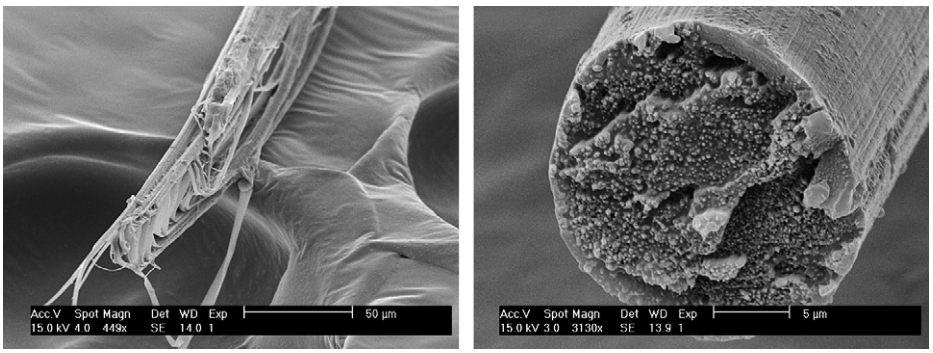

Fig. 13. Fracture surfaces of a PPTA fiber (left) and block copolymer fiber #4 (right).

enhanced and will probably improve tendency towards fibrillation of the PPTA domains and therefore increase the strength.

4. Conclusions

Uniaxially oriented films have been prepared from a series of four rod-coil block copolyamides comprised of alternating blocks of PPTA and PA 6,6. WAXS measurements made clear that copolymer films with a fraction of rigid aramids of at least 0.5 exhibit LC behaviour if the concentration of the precursor solutions was at least 15 wt% in sulphuric acid. The mechanical properties of the sheared LC films are not superior to the properties of isotropic films. The reason for this is that orientational order of the LC films is not yet high enough for the mechanical properties to benefit from the LC behaviour.

According to the tensile tests, the Young's modulus of the copolymers films increases gradually and the elongation at break decreases with increasing aramid content whereas the tensile strength remains more or less unaltered. From DMA it was clear that the thermostability of the copolymers significantly increases with increasing aramid content. This is expressed by a remarkable increase of the T_g compared to normal PA 6,6 and a storage modulus of more than 1 GPa up to at least 350 °C for copolymers with an aramid fraction of 0.5 or more. The presence of a plateau value of the modulus above the melting point of the soft block is typical for segmented block copolymers and suggest a microphase-separated structure where the rigid blocks act as covalent crosslinks between the flexible domains.

Fibers have been prepared according to a dry-jet wet spinning process of a lyotropic multiblock copolymer of alternating blocks of PPTA and PA 6,6. The average degree of polymerisation of both blocks was 10. A series of five fibers were spun from liquid crystalline solutions in sulphuric acid and the only variable parameter during the spinning process was the applied draw-ratio. All fibers displayed a significant degree of alignment and the observed orientation, the Young's modulus and the strength of the fibers increases rapidly with increasing draw-ratio. The observed modulus of the fibers can be modelled nicely with a mechanical model developed by Northolt and Van der Hout [19], which relates the initial modulus to the overall orientation in the fiber. One of the fibers was subjected to heat treatment at 300 °C what resulted in a drastic increase of the Young's modulus and a decrease in the elongation at break. These heat-treated fibers exhibited a strength of about 800 MPa, an initial Young's modulus of 55 GPa whereas an elongation at break of 2.0% was obtained.

Acknowledgements

The authors would like to acknowledge W.H.J. Nijenhuis and M.H.M Meeuwsen (both Teijin Twaron) for performing the fibers spinning experiments and J.H.M. Quaijtaal and N.A.N. Tops (both Teijin Twaron) for performing tensile testing experiments and heat treatment. The research described here is part of the research program of FOM (Fundemental Onderzoek der Materie/Fundamental Research on Matter) in the Evolution of the Microstructure of Materials (EMM), project number EMM14.

References

[1] Krigbaum WR, Preston J, Ciferri A, Zhang SF. J Polym Sci Part A Polym Chem 1987;25:653–67.
[2] Krigbaum WR, Shufan Z, Preston J, Ciferri A, Conio G. J Polym Sci Part B Polym Phys 1987;25:1043–55.
[3] Cavalleri P, Ciferri A, Dell'Erba C, Novi M, Purevsuren B. Macromolecules 1997;30:3513–8.
[4] Cavalleri P, Ciferri A, Dell'Erba C, Gabellini A, Novi M. Macromol Chem Phys 1998;199:2087–94.
[5] Fischer H, Berger W, Scheller D. Acta Polym 1994;45:88–92.
[6] Helgee B, Flodin P. Polymer 1992;33:3616–20.
[7] De Ruijter C, Jager WF, Groenewold J, Picken SJ. Macromolecules 2006;39:3824–9.
[8] De Ruijter C, Jager WF, Li L, Picken SJ. Macromolecules 2006;39:4411–7.
[9] Goto T, Maeda M, Hibi A. J Appl Polym Sci 1989;37:867–75.
[10] Northolt MG. Eur Polym J 1974;10:799–804.
[11] Haraguchi K, Kajiyama M, Takayanagi M. J Appl Polym Sci 1979;23:915–26.
[12] Bunn CW, Garner EV. Proc R Soc London Ser A 1947;189:39.
[13] Zannoni C. In: Luckhorst GR, Gray GW, editors. The molecular physics of liquid crystals. London: Academic Press; 1979 [chapter 3].
[14] Northolt MG. Polymer 1980;21:1199–204.
[15] Hindeleh AM, Halim NA, Ziq KA. J Macromol Sci Phys B 1984;23:289–309.
[16] Maier W, Saupe A. Z Naturforsch A 1961;16:816–24.
[17] Roerdink E, Warnier JMM. Polymer 1985;26:1582–8.
[18] Picken SJ, Van der Zwaag S, Northolt MG. Polymer 1992;33:2998–3006.
[19] Northolt MG, Van der Hout R. Polymer 1985;26:310–6.
[20] Yang HH. Kevlar aramid fiber. Chischester: Wiley; 1993. p. 95.
[21] Deteresa SJ, Allen SR, Farris RJ, Porter RS. J Mater Sci 1984;19:57–72.
[22] Magat EE, Morrison RE. J Polym Sci Polym Symp 1975;51:203–27.
[23] Kwolek SL, Morgan PW, Schaefgen JR, Gulrich LW. Macromolecules 1977;10:1390–6.
[24] Bair TI, Morgan PW, Killian FL. Macromolecules 1977;10:1396–400.
[25] Northolt MG, den Decker P, Picken SJ, Baltussen JJM, Schlatmann R. Adv Polym Sci 2005;178:1–108.